Rectal organoid morphology analysis (ROMA) as a promising diagnostic tool in cystic fibrosis

Senne Cuyx ,[1,2] Anabela Santo Ramalho ,[1] Nikky Corthout,[3,4] Steffen Fieuws,[5,6] Eva Fürstová,[7] Kaline Arnauts,[8,9] Marc Ferrante,[8,10] Catherine Verfaillie,[9] Sebastian Munck,[3,4] Mieke Boon,[1,2] Marijke Proesmans,[1,2] Lieven Dupont,[11,12] Kris De Boeck,[1,2] François Vermeulen ,[1,2] On behalf of the Belgian Organoid Project

For numbered affiliations see end of article.

Correspondence to
Dr François Vermeulen, Department of Development and Regeneration, Woman and Child Unit, CF research lab, KU Leuven, Leuven, Flanders, Belgium; francois.vermeulen@uzleuven.be

Received 13 October 2020
Revised 3 February 2021
Accepted 9 March 2021

To cite: Cuyx S, Ramalho AS, Corthout N, *et al*. *Thorax* Epub ahead of print: [*please include* Day Month Year]. doi:10.1136/thoraxjnl-2020-216368

ABSTRACT

Diagnosing cystic fibrosis (CF) when sweat chloride is not in the CF range and less than 2 disease-causing *CFTR* mutations are found requires physiological CFTR assays, which are not always feasible or available. We developed a new physiological CFTR assay based on the morphological differences between rectal organoids from subjects with and without CF. In organoids from 167 subjects with and 22 without CF, two parameters derived from a semi-automated image analysis protocol (rectal organoid morphology analysis, ROMA) fully discriminated CF subjects with two disease-causing mutations from non-CF subjects (p<0.001). ROMA, feasible at all ages, can be centralised to improve standardisation.

INTRODUCTION

The diagnosis of cystic fibrosis (CF), an autosomal recessive disease caused by CF transmembrane conductance regulator (*CFTR*) gene mutations, relies on abnormal (≥60 mmol/L) sweat chloride concentration (SCC) and/or two disease-causing *CFTR* mutations, as defined by the CFTR2 database.[1 2] In some subjects either with CF compatible symptoms or after neonatal screening, the diagnosis cannot be confirmed nor excluded. For patients with only intermediately elevated (30–60 mmol/L) SCC and *CFTR* mutation(s) of varying or unknown clinical consequence, second-line diagnostic tests (nasal potential difference (NPD) and intestinal current measurements (ICM)) are advocated to further explore CFTR function and assist the diagnosis. These tests are not readily available nor feasible at all ages.[1]

Rectal organoids are 3D structures grown from intestinal stem cells in a mucosal sample obtained through rectal biopsy. CFTR protein expression is maintained in and determines the morphology of these organoids, inducing swelling of non-CF organoids through salt and water accumulation in the lumen surrounded by a cellular layer, while CF organoids have no lumen as described by the Beekman group.[3 4]

We quantified morphological differences to explore the ability of rectal organoid morphology analysis (ROMA) to differentiate organoids from subjects with a clear-cut diagnosis of CF from those of subjects without CF, giving proof of concept for ROMA as a diagnostic test for CF.

METHODS

Organoids from a convenience cohort of 212 subjects were collected and imaged by one researcher blinded to subject characteristics. Twenty-three subjects were excluded due to low-quality images. Organoids of 167 subjects with CF and two disease-causing *CFTR* mutations[2] and 22 non-CF subjects were analysed (online supplemental file 1 and 2.1).

Rectal biopsies and organoid cultures were performed as previously described (online supplemental file 2.2).[4] No adverse events were reported. In total, 32 wells per subject were plated under basal conditions (no CFTR modulators nor forskolin added) and images of each well were acquired after overnight growth and calcein staining.

Two indices were calculated using imaging software (NIS-Elements AR Analysis 5.02.00) to quantify organoid morphology: the intensity ratio (IR) measures the presence or absence of a central lumen, and the circularity index (CI) quantifies the roundness of the organoids (figure 1 and online supplemental file 2.3).

Discriminant analysis was applied to differentiate between CF and non-CF subjects using IR and CI. Mann-Whitney and Fisher exact tests were used for between-group comparisons.

RESULTS

The IR and CI differed (p<0.001) between CF and non-CF (table 1). Perfect discrimination (AUC=1) was obtained with a linear discriminant analysis (figure 2). Analysis of only eight wells chosen randomly out of the 32 showed almost identical results (AUC=1) (online supplemental file 2.4).

No correlation between ROMA indexes and age was found, nor differences in IR and CI between subjects with CF in the lowest versus three highest SCC quartiles (<87 and ≥87 mmol/L, respectively). The IR (p=0.007), but not CI (p=0.419), was different between PI (pancreatic insufficient) and PS (pancreatic sufficient) subjects with CF. For additional statistical analyses, see online supplemental files 2.4 and 3.

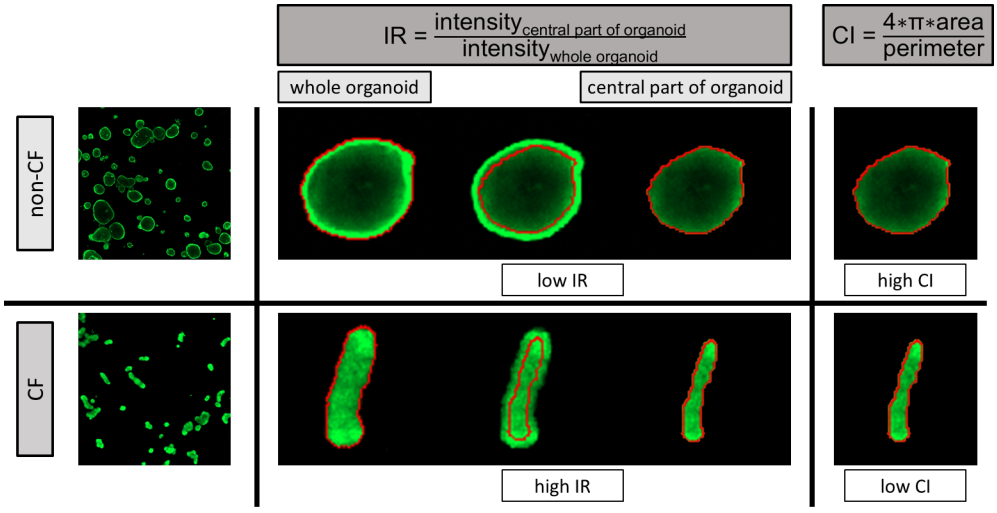

Figure 1 Images of rectal organoids from subjects without (upper panels) and with CF (lower panels). Illustration of the methods to calculate the two indexes, IR (intensity ratio; central panel) and CI (circularity index; right panel), used to quantify morphological differences between rectal organoids of subjects with and without CF. IR measures the presence or absence of a central lumen, calculated in three steps: (1) calculate the global fluorescence intensity of the organoids: erode 1 pixel (2.5 µm) to remove the surrounding 'halo' around each structure and measure the mean fluorescence intensity of the remaining whole organoid; (2) calculate the lumen fluorescence intensity of the organoids: erode 10 pixels from each structure to remove the cellular border from the organoids and measure the mean fluorescence intensity of the remaining structure; (3) IR is equal to (intensity central part of organoid)/(intensity whole organoid) and is higher in CF than in non-CF organoids. CI quantifies the roundness of the organoids, defined as (4×π×area)/perimeter, which is lower in CF than in non-CF organoids. CF, cystic fibrosis; IR, intensity ratio; CI, circularity index.

DISCUSSION

Both IR and CI, calculated with ROMA, discriminated subjects with clinical CF and two disease-causing *CFTR* mutations from non-CF subjects. This makes ROMA appealing as an additional physiological CFTR assay to assist in the diagnosis of CF, with a discriminative ability comparable with that reported for SCC and other physiological CFTR assays such as NPD or ICM.[5 6]

Similarly to SCC,[5] mean IR is different between PS and PI subjects with CF, although not fully discriminative. Residual CFTR function, translating in pancreatic sufficiency, leads to the presence of a small lumen in the organoids and thus lower IR, without altering the organoids' irregular shape quantified by CI.

The current study is monocentric and needs replication, but samples have already been successfully received from other Belgian and international centres. Before ROMA can be proposed as diagnostic test for CF, more data are needed, especially from patients with a clinical CF diagnosis but without two disease-causing *CFTR* mutations, and from prospective analysis in subjects with unresolved CF diagnosis, including infants with CF screening positive, inconclusive diagnosis (CFSPID). The absence of a gold standard will need to be taken into account, as with other CFTR physiological assays.

Rectal suction biopsy for ROMA can easily be performed in general hospitals with low complication rates,[7] even in infants (with CFSPID). Quality requirements for biopsies are lower for ROMA[8] than for ICM,[9] as only the presence of viable crypts is needed to grow an organoid culture, rather than an intact epithelium required for electrophysiology. Biopsies can thus be shipped to a central laboratory for analysis,[8] which ensures standardisation together with the semi-automated nature of the analysis.

Possible issues with ROMA include the complexity and cost of organoid culture. However, standardised protocols are available for organoid culture and technique portability has been demonstrated.[8] Reducing the number of wells from 32 to 8 resulted in virtually identical results and would make ROMA more cost-efficient. Using rectal instead of airway tissue is both an advantage (CFTR specific, no influence of disease state)[1] and a disadvantage (possible differences in CFTR function between organs). The delay of 1–2 months between taking the biopsy and availability of results is rarely an issue as these cases are often not urgent. This waiting time is similar to that of extensive genetic analysis.

Further work will have to assess ROMA as a diagnostic test

Table 1 Baseline characteristics of the subjects and indexes calculated using rectal organoid morphology analysis (ROMA)

	CF	Non-CF	p value
n	167	22*	
IR	1.11 (0.93–1.34)	0.76 (0.61–0.88)	<0.001
CI	0.59 (0.49–0.70)	0.79 (0.73–0.84)	<0.001
Age (years)	18 (0–60)	44 (0–77)	<0.001
Gender	85 male (51%)	11 male (50%)	>0.999
	82 female (49%)	11 female (50%)	
SCC (mmol/L) (n=164)	97.61 (36–160)		
SCC low (<87 mmol/L) or high (≥87 mmol/L)	41 low (25%)		
	123 high (75%)		
Pancreatic status (n=165)	28 PS (17%)		
	137 PI (83%)		

n or mean and range.
*7 carriers, 3 non-carriers, 2 autosomal dominant polycystic kidney disease, 6 ulcerative colitis, 1 polyp screening, 3 healthy controls included in a study about inflammatory bowel disease.
CF, cystic fibrosis; IR, intensity ratio; CI, circularity index; SCC, sweat chloride concentration; PI, pancreatic insufficient; PS, pancreatic sufficient

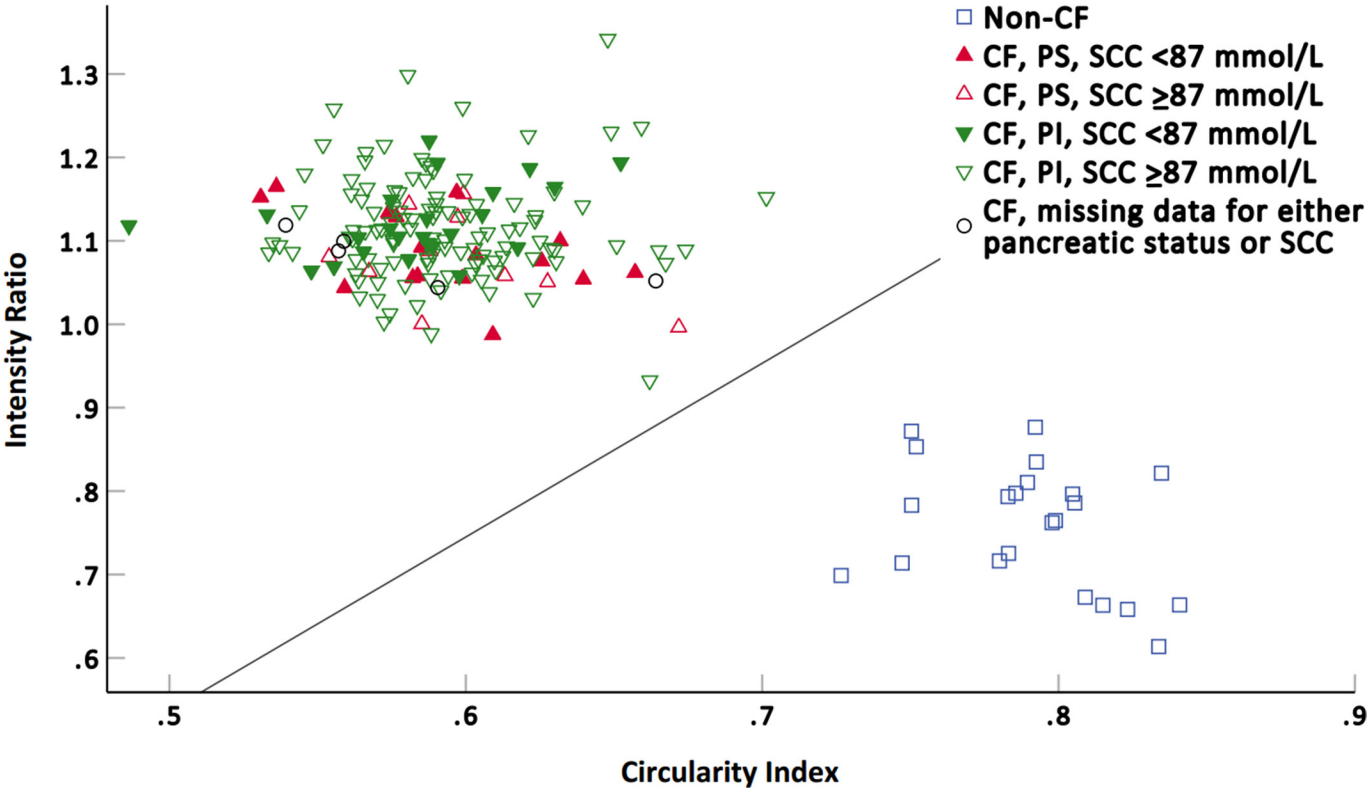

Figure 2 Intensity ratio (IR) and circularity index (CI) values of each subject according to disease status, pancreatic status and sweat chloride concentration. The line represents the optimal discrimination line obtained by linear discriminant analysis. CF, cystic fibrosis; PI, pancreatic insufficient; PS, pancreatic sufficient; SCC, sweat chloride concentration.

in patients with equivocal diagnosis. Beyond diagnosis, organoids used for ROMA can be biobanked for later personalised medicine research for the newly diagnosed patients with CF.[10] ROMA could also contribute to measuring modulator efficiency, as restoring CFTR function to high levels causes the appearance, before any stimulation, of a central lumen and swelling to a more round shape,[3 4] measured by IR and CI, respectively.

Author affiliations
[1]Department of Development and Regeneration, Woman and Child Unit, CF Research Lab, KU Leuven, Leuven, Flanders, Belgium
[2]Department of Pediatrics, Pediatric Pulmonology, University Hospital of Leuven, Leuven, Flanders, Belgium
[3]VIB Bio Imaging Core, VIB KU Leuven Center for Brain & Disease Research, Leuven, Belgium
[4]Department for Neuroscience, KU Leuven, Leuven, Flanders, Belgium
[5]Interuniversity Center for Biostatistics and Statistical Bioinformatics, KU Leuven, Leuven, Flanders, Belgium
[6]Interuniversity Center for Biostatistics and Statistical Bioinformatics, Hasselt University, Hasselt, Limburg, Belgium
[7]Department of Pediatrics, 2nd Faculty of Medicine, Motol University Hospital, Praha, Czech Republic
[8]Department of Chronic Diseases and Metabolism (CHROMETA), Translational Research Center for Gastrointestinal Disorders (TARGID), KU Leuven, Leuven, Flanders, Belgium
[9]Department of Development and Regeneration, Stem Cell Institute Leuven (SCIL), KU Leuven, Leuven, Flanders, Belgium
[10]Department of Gastroenterology and Hepatology, University Hospital of Leuven, Leuven, Flanders, Belgium
[11]Department of Chronic Diseases, Metabolism and Ageing; Pneumology, University Hospital of Leuven, Leuven, Flanders, Belgium
[12]Department of Respiratory Diseases, University Hospital of Leuven, Leuven, Flanders, Belgium

Acknowledgements We thank the patients and parents who participated in this study. We thank Els Aertgeerts, Karolien Bruneel, Claire Collard, Liliane Collignon, Monique Delfosse, Anja Delporte, Nathalie Feyaerts, Cécile Lambremont, Lut Nieuwborg, Nathalie Peeters, Ann Raman, Pim Sansen, Hilde Stevens, Marianne Schulte, Els Van Ransbeeck, Christel Van de Brande, Greet Van den Eynde, Marleen Vanderkerken, Inge Van Dijck, Audrey Wagener, Monika Waskiewicz and Bernard Wenderickx for logistic support. We also thank Stefan Joris and Dr. Jan Vanleeuwe from the Mucovereniging/Association Muco for their support.

Collaborators Belgian Organoid Project: Hedwige Boboli (CHR Citadelle, Liège, Belgium), Linda Boulanger (University Hospital Leuven, Belgium), Georges Casimir (HUDERF, Brussels, Belgium), Benedicte De Meyere (University Hospital Ghent, Belgium), Elke De Wachter (University Hospital Brussels, Belgium), Danny De Looze (University Hospital Ghent, Belgium), Isabelle Etienne (CHU Erasme, Brussels, Belgium), Laurence Hanssens (HUDERF, Brussels), Christiane Knoop (CHU Erasme, Brussels, Belgium), Monique Lequesne (University Hospital Antwerp, Belgium), Vicky Nowé (GZA St. Vincentius Hospital Antwerp), Dirk Staessen (GZA St. Vincentius Hospital Antwerp), Stephanie Van Biervliet (University Hospital Ghent, Belgium), Eva Van Braeckel (University Hospital Ghent, Belgium), Kim Van Hoorenbeeck (University Hospital Antwerp, Belgium), Eef Vanderhelst (University Hospital Brussels, Belgium), Stijn Verhulst (University Hospital Antwerp, Belgium), Stefanie Vincken (University Hospital Brussels, Belgium).

Contributors Conceptualisation: SC, ASR, FV and KDB. Methodology: SC, ASR, NC, SM, KDB and FV. Recruiting of CF subjects and collection of rectal biopsies: MB, MP, FV and LD. Recruiting of control subjects and collection of rectal biopsies: MB, MP, FV, LD, KA and MF. Culturing the organoids and performing the rectal organoid morphology analysis: SC, EF and ASR. Analysis of the results and figures preparation: SC, ASR, SF and FV. Writing—original draft: SC, ASR and FV. Writing—review and editing: SC, ASR, NC, SF, EF, KA, MF, CV, SM, MB, MP, LD, KDB, FV, HB, LB, GC, BDM, EDW, DDL, IE, LH, CK, ML, VN, DS, SVB, EVB, KVH, EV, SVe, SVi. Supervision: ASR, FV and KDB.

Funding This study was funded by the Belgian CF patients' association "Mucovereniging/Association Muco", the Research Grant of the Belgian Society of Paediatrics BVK-SBP 2019, and a grant from the UZ Leuven Fund for Translational Biomedical Research.

Competing interests None declared.

Patient consent for publication Not required.

Ethics approval Approval from the Ethical committee of UZ Leuven and informed consent from all subjects or representatives were obtained.

Provenance and peer review Not commissioned; externally peer reviewed.

ORCID iDs
Senne Cuyx http://orcid.org/0000-0002-6473-8966
Anabela Santo Ramalho http://orcid.org/0000-0003-3143-3661
François Vermeulen http://orcid.org/0000-0003-2303-2470

REFERENCES

1 De Boeck K, Vermeulen F, Dupont L. The diagnosis of cystic fibrosis. *La Presse Médicale* 2017;46:e97–108.
2 CFTR2 [Internet]. Available: https://www.cftr2.org/ [Accessed cited 2019 May 30].
3 Dekkers JF, Wiegerinck CL, de Jonge HR, *et al*. A functional CFTR assay using primary cystic fibrosis intestinal organoids. *Nat Med* 2013;19:939–45 https://pubmed.ncbi.nlm.nih.gov/23727931/
4 Dekkers JF, Berkers G, Kruisselbrink E, *et al*. Characterizing responses to CFTR-modulating drugs using rectal organoids derived from subjects with cystic fibrosis. *Sci Transl Med* 2016;8:344ra84 https://pubmed.ncbi.nlm.nih.gov/27334259/
5 Wilschanski M, Dupuis A, Ellis L, *et al*. Mutations in the cystic fibrosis transmembrane regulator gene and in vivo transepithelial potentials. *Am J Respir Crit Care Med* 2006;174:787–94 https://pubmed.ncbi.nlm.nih.gov/16840743/
6 Derichs N, Sanz J, Von Kanel T, *et al*. Intestinal current measurement for diagnostic classification of patients with questionable cystic fibrosis: validation and reference data. *Thorax* 2010;65:594–9 http://www.ncbi.nlm.nih.gov/pubmed/20627915
7 Friedmacher F, Puri P. Rectal suction biopsy for the diagnosis of Hirschsprung's disease: a systematic review of diagnostic accuracy and complications. *Pediatr Surg Int* 2015;31:821–30 https://link.springer.com/article/
8 Vonk AM, van Mourik P, Ramalho AS, *et al*. Protocol for application, standardization and validation of the forskolin-induced swelling assay in cystic fibrosis human colon organoids. *STAR Protoc* 2020;1:100019.
9 Servidoni MF, Sousa M, Vinagre AM, *et al*. Rectal forceps biopsy procedure in cystic fibrosis: technical aspects and patients perspective for clinical trials feasibility. *BMC Gastroenterol* 2013;13:91.
10 Ramalho AS, Fürstová E, Vonk AM. Correction of CFTR function in intestinal organoids to guide treatment of cystic fibrosis. *Eur Respir J [Internet]* 2020.

Supplements

Supplement 1: STARD flow diagram

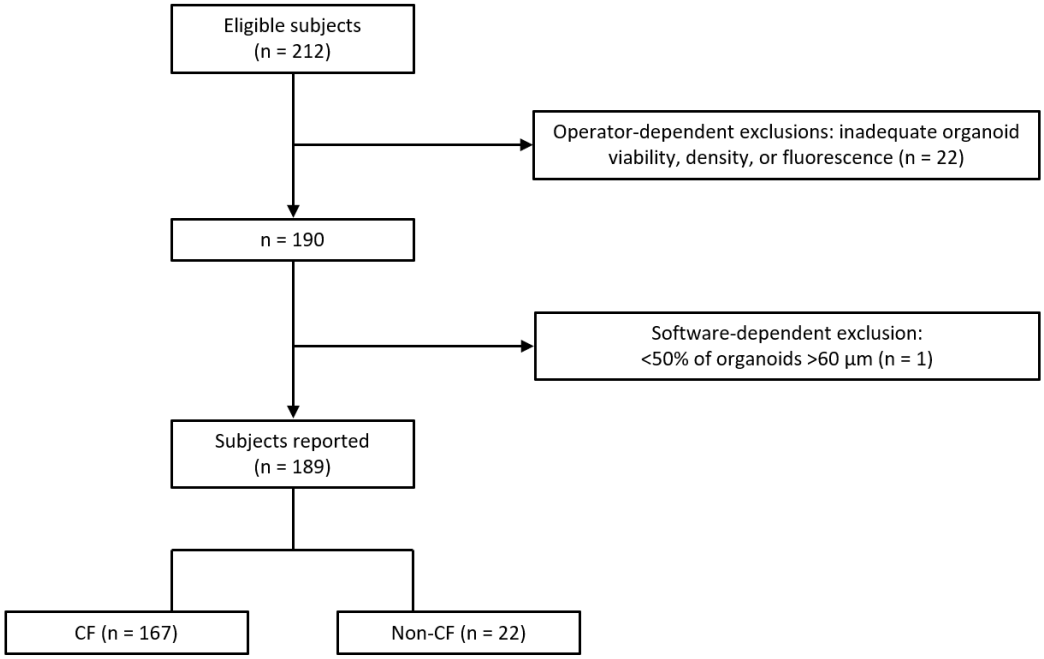

Supplementary figure 1: STARD flow diagram

Supplement 2: Supplementary methods

2.1) Quality criteria for exclusion of organoid cultures

Exclusion criteria for organoid images	
Determined by the operator	**Determined by the software**
Many differentiated or dead structures or debris	Less than 50% of structures >60 µm (organoids should be large enough to show morphology typical to either CF or non-CF)
Inadequate plating density: too many (eg. overlapping) or too few organoids	<500 or >3000 organoids (defined as structures >40 µm) in 32 wells; <125 or >750 organoids in 8 wells
Inadequate fluorescence distribution (organoids not clearly delineated, background signal too high)	

Supplementary table 1: quality criteria for exclusion of organoid cultures

2.2) Plating of organoids and image acquisition

Organoids were plated in 32 wells of a 96 well plate, left to incubate overnight (16-24 hours) without CFTR modulators or forskolin, and stained with calcein green 0.6 µM. The plate was then transferred to a LMS800 Zeiss confocal microscope with an automated stage and integrated incubator. The x/y position and the best focus (z position) of the organoids in each well were manually defined. Images were then automatically acquired in a unidirectional way using a 5x objective with a resolution of 1024x1024 pixels (pixel size 2.5x2.5 µm) and 16 bits depth. Zen blue software (v2.6 from Zeiss) was used. The 32 images per subject were exported as TIFF files and analysed in the NIS-Elements Advanced Research Analysis Imaging Software (v.5.02.00) according to the table below.

2.3) Semi-automated image analysis protocol

A semi-automated protocol was used for image analysis, in which the number of organoids (defined as structures ≥40 µm) was counted, as well as the number of organoids which had grown enough to show the typical CF or non-CF morphology (defined as structures ≥60 µm). The exclusion of organoids ≥40 and <60 µm was based on separate analysis of this subset, showing no significant morphological differences for these small structures between CF and non-CF subjects (round and dense in both cases). Two erosion steps were performed on all included structures to analyse the whole organoid and the central part separately. Two indices were calculated to quantify organoid morphology (figure 2).

Semi-automated protocol for image analysis in NIS-Elements Advanced Research Analysis Imaging Software (v.5.02.00)	
Procedure	Rationale
Make one Network Data (.ND) file of all 32 pictures for each subject	Enables simultaneous analysis of all 32 pictures per subject
Recalibrate images so 1 pixel is 2.5x2.5 µm ("recalibrate document" function)	Enables erosions in µm instead of pixels
Delineate structures with a lower intensity threshold of 4500 and an upper threshold of 65535 ("define threshold" function); "smooth" and "clean" functions off; “fill holes” function on; "separate" function on x3	Delineates fluorescent structures, including the lumen if present
Select all structures ≥40 µm and count ("size" parameter)	Counts the total number of organoids in the 32 wells, excludes small debris
Select all structures ≥60 µm and count ("size" parameter)	Counts the organoids large enough to show morphology typical to either CF or non-CF
Remove all structures touching the borders of the picture ("remove objects touching border" function)	Removes organoids that are not completely visible, as their morphology cannot be accurately quantified
Erode 1 pixel (=2.5 µm) from the border of each ≥60 µm structure ("erode" function)	Removes the “halo” of background fluorescence surrounding the organoids
Measure the mean intensity of each structure	Measures the mean fluorescence of the whole organoids
Erode 10 pixels (=25 µm) from the border of each original ≥60 µm structure ("erode" function)	In non-CF organoids, this erodes the cellular border and leaves only the lumen
	In CF organoids, this erodes the outer part of the organoid, which has roughly the same intensity as the inner part that remains
Measure the mean intensity of each structure	Measures the mean fluorescence of the central part of the organoids
Measure the circularity of each structure	Measures the mean circularity of the organoids

Supplementary table 2: semi-automated protocol for image analysis

2.4) Statistical methods and additional analyses

Linear discriminant analysis and quadratic discriminant analysis were used to discriminate between subjects with and without CF using IR and CI indexes. The area under the ROC curve (AUC) was reported. A bootstrap approach was used to obtain a 95% confidence interval for this AUC and to estimate the degree of overoptimism in its quantification. Indeed, the observed AUC overestimates the future performance since the same data were used to construct and evaluate the model. Given that the data are sparse at the intersection of both groups, a parametric resampling procedure was preferred to a non-parametric version to quantify the degree of overoptimism in the estimation of the AUC.

Step 1: sample a mean vector and a covariance matrix (for IR and CI) from the observed mean and covariance.

Step 2: draw N0 controls and N1 cases, with N0 and N1 the observed number of controls and cases, respectively. They form one bootstrap sample.

Step 3: calculate the AUC in the bootstrap sample and the AUC in the original dataset based on the model in the bootstrap sample.

Repeat step 1 to step 3 1000 times.

Step 4: calculate the mean AUC of the 1000 bootstrap samples and the mean AUC of the 1000 evaluations in the original dataset. The difference is the estimate of overoptimism. Subtract this estimate from the observed AUC to get the optimism-corrected AUC.

Perfect discrimination (AUC=1) between CF and non-CF using IR and CI was obtained with linear as well as with quadratic discriminant analysis. Perfect discrimination was also obtained in all bootstrap samples (hence, the lower limit of the confidence interval also equals 1). The AUC corrected for overoptimism equalled 0.9879132 and 0.9998538, respectively.

These analyses were performed using SAS software, version 9.4 of the SAS System for Windows.

Supplementary figure 2: Results for linear (upper panel) and quadratic (lower panel) discriminant analysis.

Discrimination lines were obtained with linear and quadratic discriminant analysis, respectively. These lines correspond to combinations of values for which the posterior probability to be a case equals 0.50 (using an equal prior probability for both classes).

CI: circularity index; IR: intensity ratio

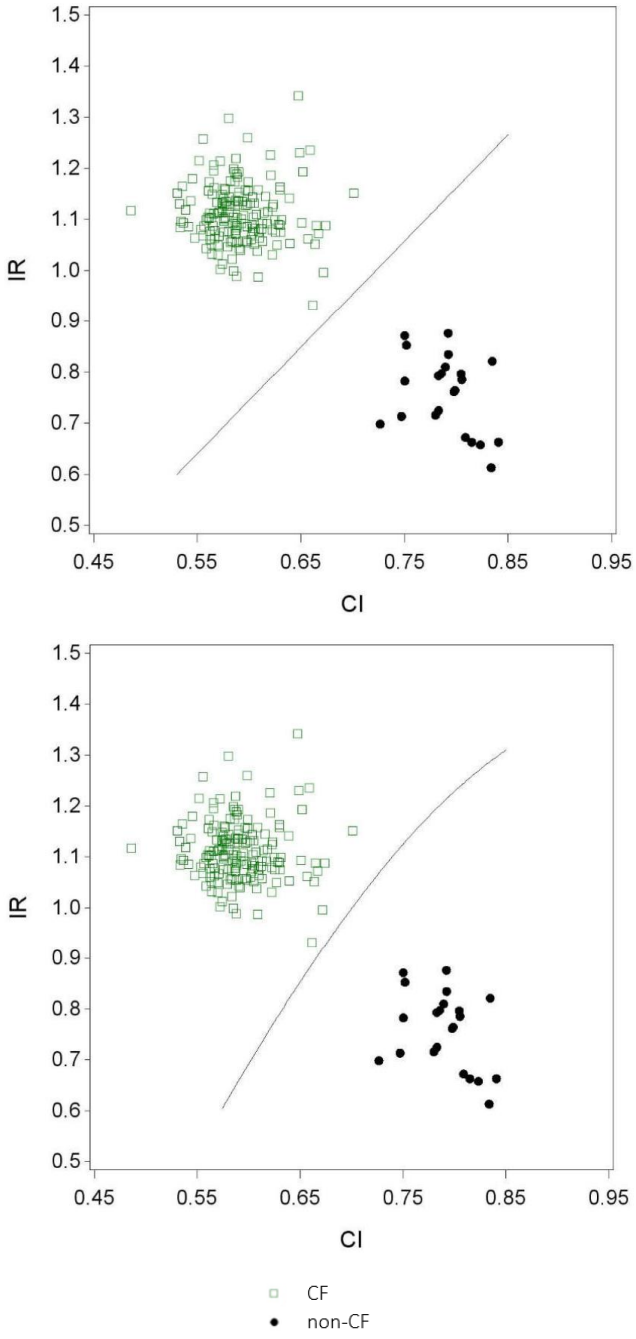

Supplementary figure 3: Discrimination lines obtained in 10 bootstrap samples for linear (upper panel) and quadratic (lower panel) discriminant analysis.
These discrimination lines give an impression of the uncertainty of the discrimination line by presenting the result in 10 bootstrap samples.
CI: circularity index; IR: intensity ratio

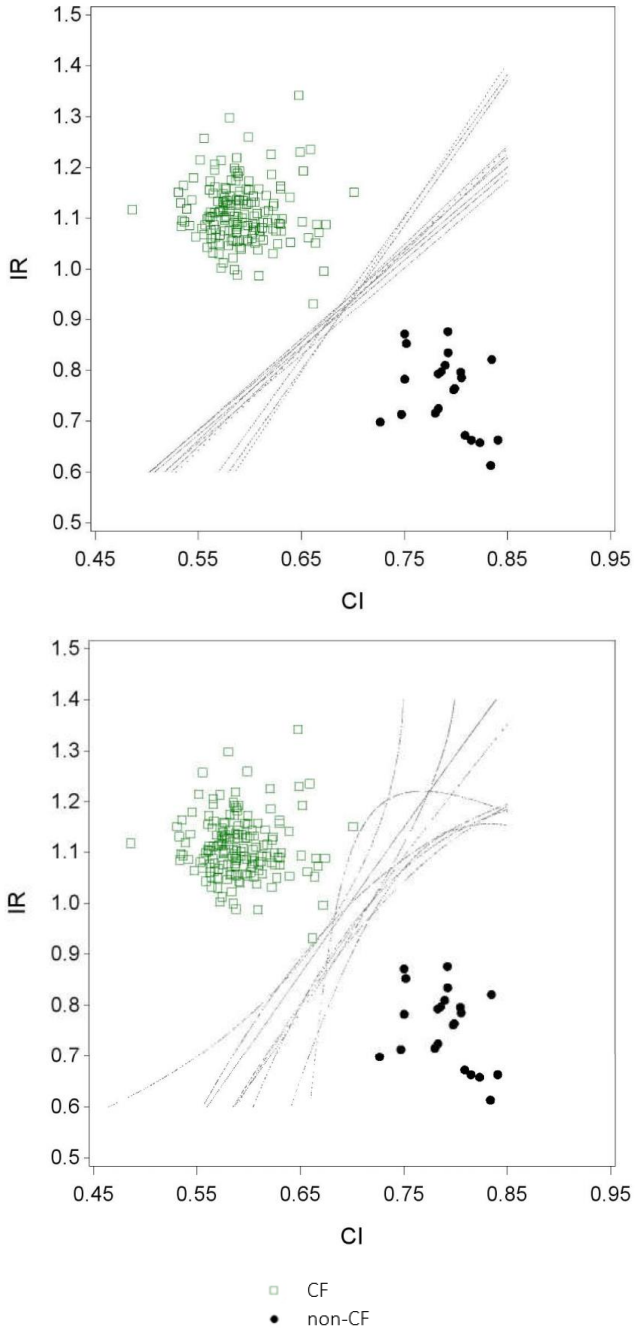

Results for data using 8 wells at random per subject and using the same statistical methodology were comparable to the results using 32 wells. Again, perfect discrimination was obtained with the linear as well as with the quadratic discriminant analysis.

Supplementary figure 4: results for linear (upper panel) and quadratic (lower panel) discriminant analysis, based on 8 wells data.
CI: circularity index; IR: intensity ratio

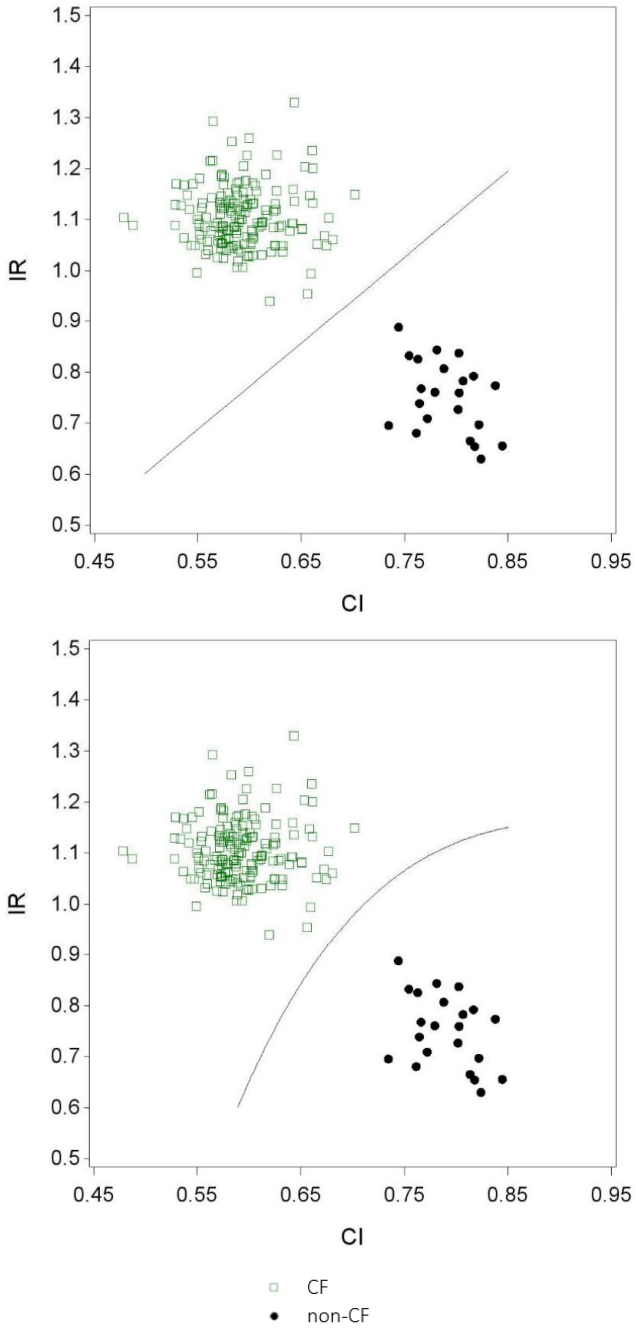

Supplementary figure 5: Discrimination lines obtained in 10 bootstrap samples, based on 8 wells data. Results for linear (upper panel) and quadratic (lower panel) discriminant analysis.
CI: circularity index; IR: intensity ratio

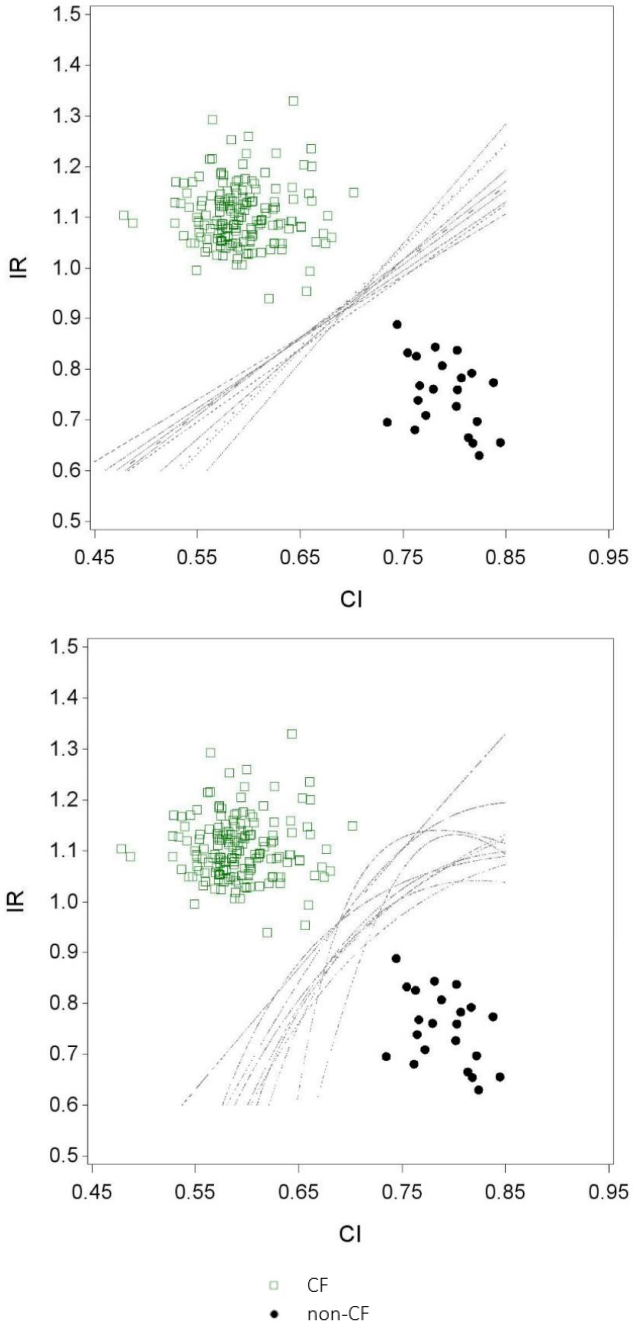

Supplement 3: Supplementary statistical tests for subgroup analysis

Additional statistical test were performed for subgroup analysis. Pearson's correlation coefficients were used to assess correlations between ROMA indexes and age, and Mann-Whitney and Fisher exact tests for between-group comparisons in IBM SPSS Statistics Version 26.

Supplementary figure 6: scatter plot with fit line for intensity ratio (IR) by age in CF subjects (Pearson's correlation coefficient *r*=-0.042 (p=0.592))

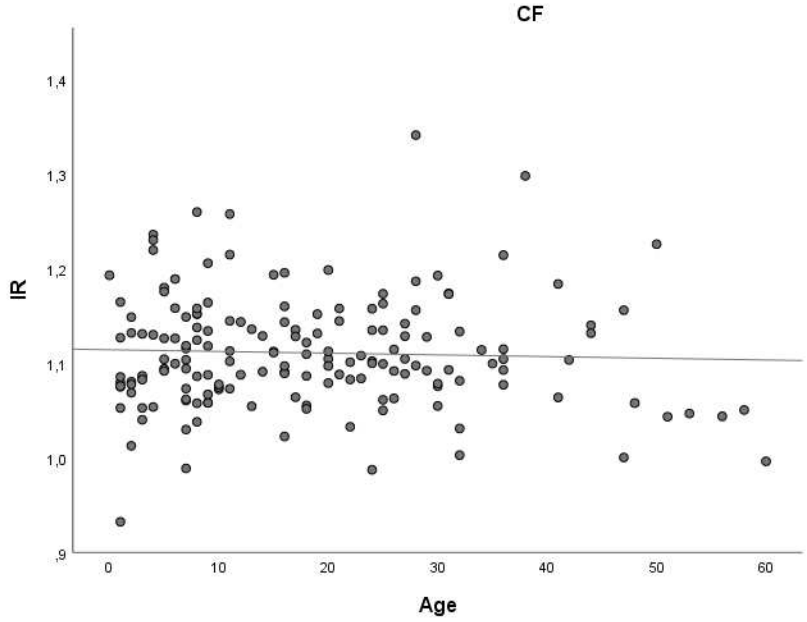

Supplementary figure 7: scatter plot with fit line for circularity index (CI) by age in CF subjects (Pearson's correlation coefficient *r*=0.060 (p=0.440))

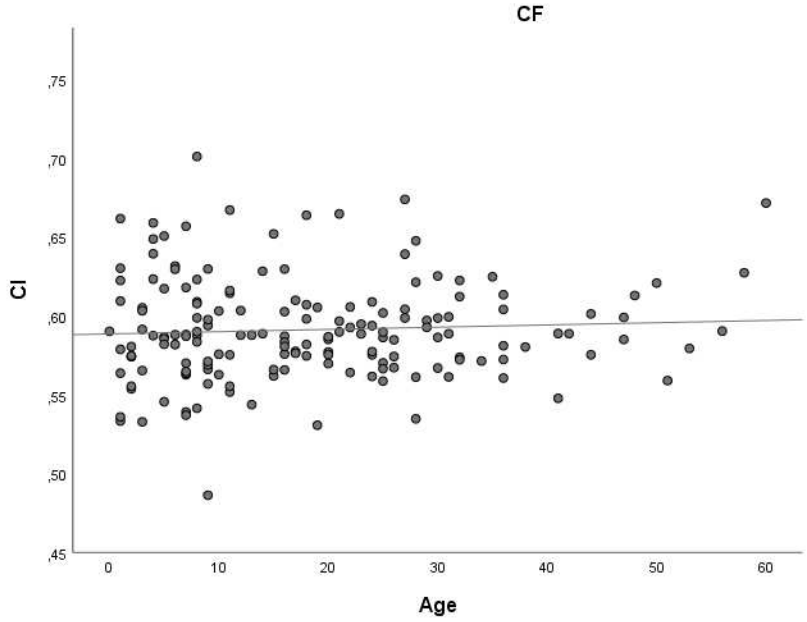

Supplementary figure 8: scatter plot with fit line for intensity ratio (IR) by age in non-CF subjects (Pearson's correlation coefficient *r*=-0.207 (p=0.356))

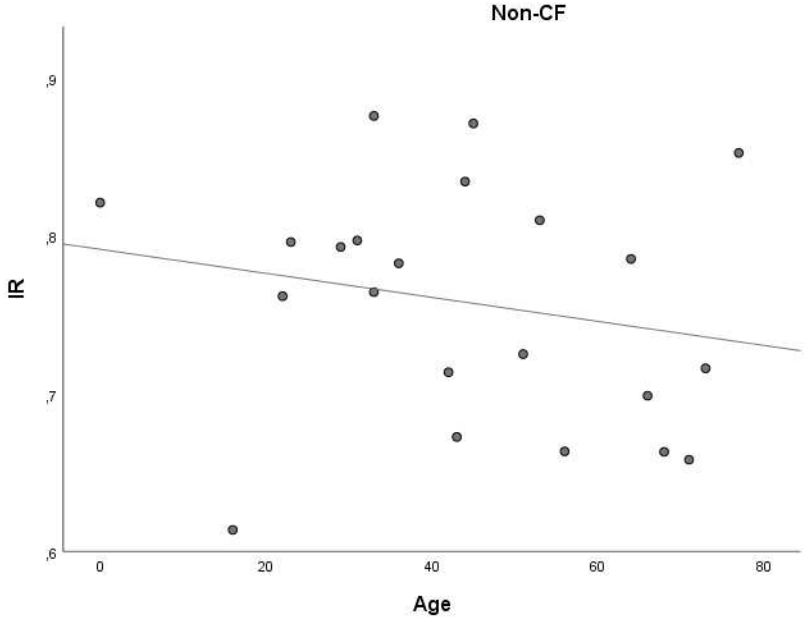

Supplementary figure 9: scatter plot with fit line for circularity index (CI) by age in non-CF subjects (Pearson's correlation coefficient *r*=-0.294 (p=0.185))

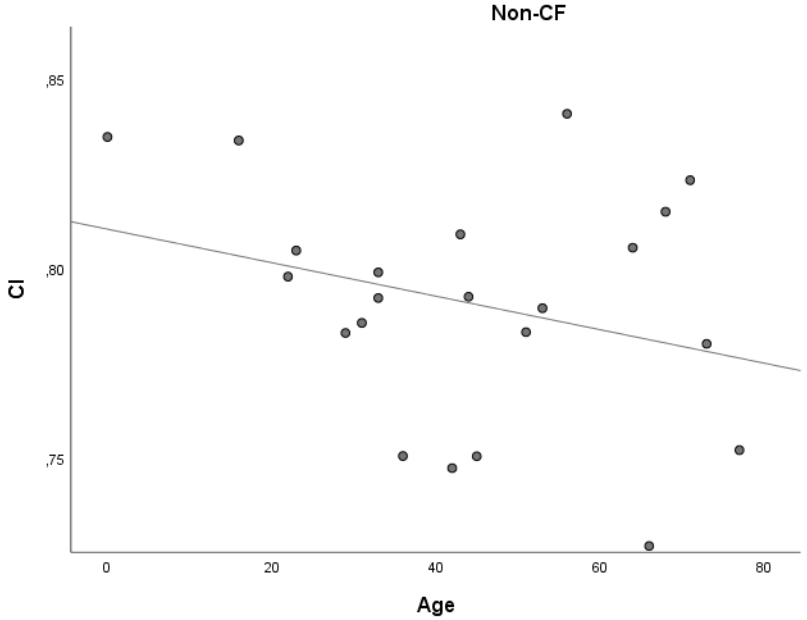

Supplementary figure 10: scatter plot with fit line for intensity ratio (IR) by age in homozygous F508del subjects (Pearson's correlation coefficient *r*=0.100 (p=0.494))

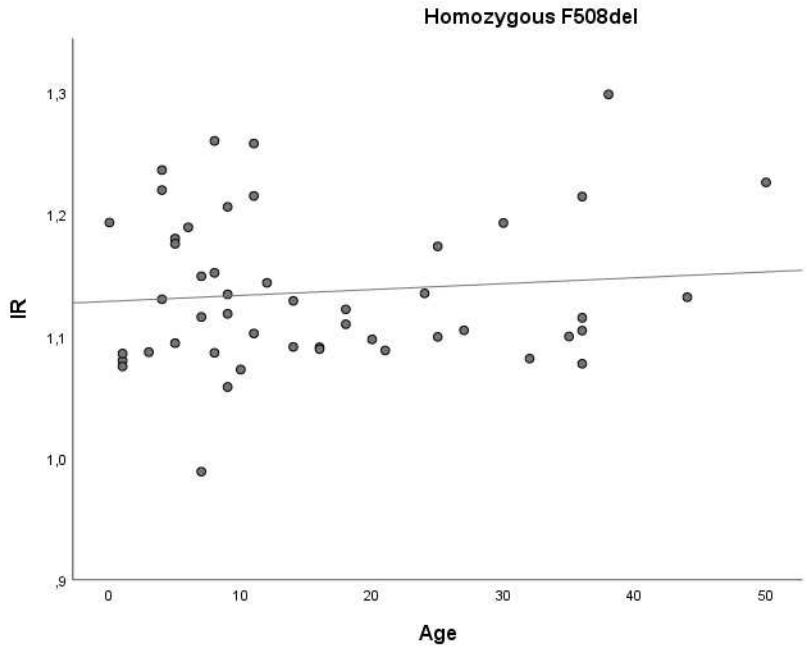

Supplementary figure 11: scatter plot with fit line for circularity index (CI) by age in homozygous F508del subjects (Pearson's correlation coefficient *r*=0.042 (p=0.777))

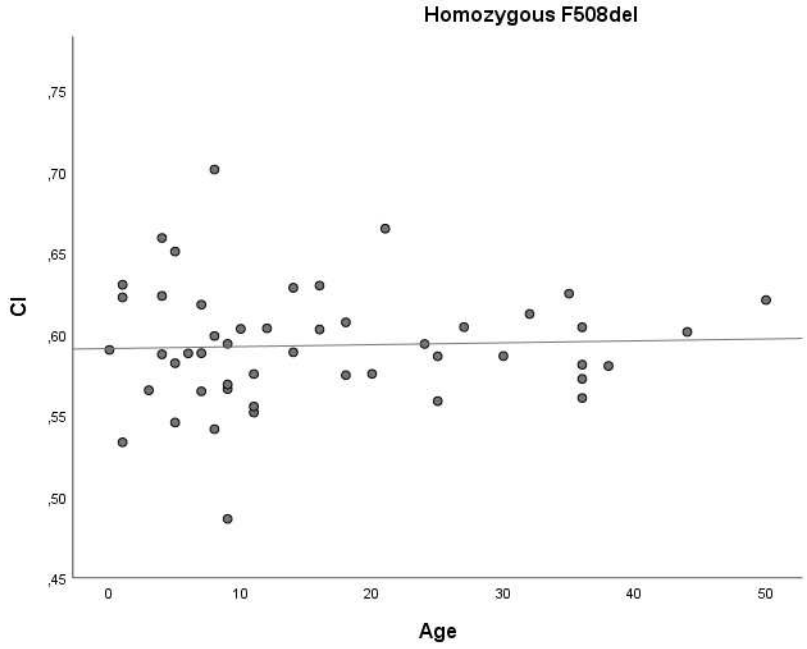

Supplementary table 3: between-group differences for subjects with pancreatic sufficiency and pancreatic insufficiency

	PS	PI	p value
n	28	137	
IR	1.084 (0.987-1.165)	1.117 (0.932-1.342)	0.007
CI	0.597 (0.531-0.672)	0.591 (0.486-0.701)	0.419
SCC low (<87 mmol/L) or high (≥87 mmol/L)	16 low (59%) 11 high (41%)	24 low (18%) 111 high (82%)	<0.001

n or mean and range

PI: pancreatic insufficient; PS: pancreatic sufficient; IR: intensity ratio; CI: circularity index; SCC: sweat chloride concentration

Supplementary table 4: between-group differences for subjects with low and high sweat chloride

	SCC <87 mmol/l	SCC ≥87 mmol/l	p value
n	41	123	
IR	1.11 (0.99-1.22)	1.11 (0.93-1.34)	0.763
CI	0.59 (0.49-0.66)	0.59 (0.53-0.70)	0.602
Pancreatic status (n = 162)	16 PS (40%) 24 PI (60%)	11 PS (9%) 111 PI ((91%)	<0.001

n or mean and range

SCC: sweat chloride concentration; IR: intensity ratio; CI: circularity index; PS: pancreatic sufficient; PI: pancreatic insufficient

Supplementary table 5: subjects ordered by genotype with age, sweat chloride concentration, pancreatic status, and ROMA indexes

Genotype	n	Range age	Range sweat chloride concentration	PS/PI	Range CI	Range IR
F508del / F508del	49	0 - 50	73,5 - 134	0 / 49	0,49 - 0,70	0,99 - 1,30
F508del / G542X	11	4 - 31	79 - 112,2	0 / 11	0,53 - 0,65	1,06 - 1,34
F508del / 3272-26A->G	8	3 - 47	65,1 - 102	5 / 3	0,53 - 0,66	1,00 - 1,16
F508del / L927P	7	2 - 24	74,1 - 160	0 / 7	0,53 - 0,62	1,05 - 1,20
F508del / N1303K	7	1 - 9	81,1 - 121	0 / 7	0,56 - 0,66	0,93 - 1,10
F508del / 1717-1G->A	4	16 - 25	74,1 - 96	0 / 4	0,57 - 0,61	1,10 - 1,16
F508del / A455E	4	6 - 60	71 - 91,1	3 / 1	0,57 - 0,67	1,00 - 1,16
F508del / E92K	3	2 - 27	117 - 137	1 / 1	0,54 - 0,64	1,08 - 1,14
F508del / 2789+5G->A	3	1 - 56	74 - 122	2 / 1	0,54 - 0,6	1,04 - 1,16
F508del / 3849+10kbC->T	3	8 - 29	36 - 113	3 / 0	0,58 - 0,6	1,06 - 1,13
1717-1G->A / L927P	2	6 - 24	97,1 - 107	0 / 2	0,56 - 0,58	1,10 - 1,13
F508del / G970R	2	1 - 20	83 - 87,1	0 / 2	0,58 - 0,61	1,08 - 1,10
F508del / I507del	2	18 - 20	87 - 114	0 / 2	0,59 - 0,60	1,08 - 1,09
F508del / R553X	2	3 - 16	88,1 - 94,1	0 / 2	0,58 - 0,59	1,02 - 1,04
F508del / S1255P	2	25 - 31	92 - 97	0 / 2	0,56 - 0,59	1,14 - 1,17
F508del / Y1092X	2	7 - 22	89,1 - 93	0 / 2	0,56 - 0,61	1,06 - 1,08
N1303K / delEx19	2	9 - 22	85,1 - 87,1	0 / 2	0,56 - 0,63	1,03 - 1,16
N1303K / N1303K	2	10 - 31	82,1 - 94,1	0 / 2	0,56 - 0,59	1,08 - 1,09
F508del / R334W	2	22 - 26	94 - 98	1 / 1	0,57 - 0,59	1,06 - 1,10
W1282X / I1234V	2	25 - 30	79 - 115	1 / 1	0,57 - 0,63	1,05 - 1,08
F508del / I336K	2	21 - 30	83 - 85	2 / 0	0,60 - 0,60	1,06 - 1,16
F508del / 182delT	1	9	59	0 / 0	0,56	1,09
1811+1.6kbA->G / 1811+1.6kbA->G	1	32	116,8	0 / 1	0,57	1,00
2143delT / G542X	1	1	110	0 / 1	0,58	1,13
2143delT / N1303K	1	9	84,89	0 / 1	0,60	1,06
3272-26A->G / L165S	1	44	99	0 / 1	0,58	1,14
394delTT / L927P	1	11	89,1	0 / 1	0,61	1,11
405+1G->A / 3121-1G->A	1	8	102	0 / 1	0,62	1,12
405+1G->A / 405+1G->A	1	27	105	0 / 1	0,67	1,09
711+1G->T / c.1819_1902del	1	13	102	0 / 1	0,59	1,05
c.1329_1350del / c.c.1329_1350del	1	2	85,1	0 / 1	0,58	1,08
F508del / 1078delT	1	15	86,1	0 / 1	0,65	1,19
F508del / 1259insA	1	17	116	0 / 1	0,58	1,14
F508del / 1898+1G->C	1	41	113	0 / 1	0,59	1,18
F508del / 394delTT	1	28	77	0 / 1	0,62	1,19
F508del / delEx19,20,21	1	10	106	0 / 1	0,58	1,08
F508del / E60X	1	34	98	0 / 1	0,57	1,11
F508del / G551D	1	32	98	0 / 1	0,62	1,03

F508del / L227R	1	13	93	0 / 1	0,54	1,14
F508del / M1101K	1	20	108	0 / 1	0,57	1,11
F508del / R352Q	1	41	59,9	0 / 1	0,55	1,06
F508del / S1251N	1	53	91	0 / 1	0,58	1,05
F508del / W1282X	1	36	106	0 / 1	0,61	1,09
F508del / W401X	1	42	121	0 / 1	0,59	1,10
G542X / G970R	1	26	85,1	0 / 1	0,57	1,11
I507del / L927P	1	7	96	0 / 1	0,54	1,09
L227R / L227R	1	1	114,5	0 / 1	0,56	1,05
L927P / L927P	1	11	89,1	0 / 1	0,67	1,07
N1303K / 1717-1G->A	1	7	111	0 / 1	0,59	1,07
N1303K / 4010del4	1	23	125	0 / 1	0,59	1,08
N1303K / Q359K/T360K	1	17	117	0 / 1	0,61	1,06
Q493X / W401X	1	5	82,1	0 / 1	0,59	1,13
R1158X / R1162X	1	16	102	0 / 1	0,58	1,16
R553X / A455E	1	7	83,1	0 / 1	0,56	1,10
W1282X / delEx2-3	1	28	130	0 / 1	0,56	1,16
W1282X / G85E	1	30	113,8	0 / 1	0,57	1,08
W1282X / W1089X	1	8	118	0 / 1	0,59	1,15
1717-1G->A / 2789+5G->A	1	7	79,1	1 / 0	0,66	1,06
2183AA->G / R347H	1	26	68,1	1 / 0	0,59	1,09
3272-26A->G / 3659delC	1	16	91,1	1 / 0	0,58	1,14
A455E / delEx1 and promoter	1	48	98	1 / 0	0,61	1,06
F508del / L138ins	1	2	108	1 / 0	0,57	1,13
F508del / R117C	1	4	46,5	1 / 0	0,64	1,05
G542X / 2789+5G->A	1	12	98,1	1 / 0	0,59	1,09
I507del / E60K	1	24	73	1 / 0	0,61	0,99
N1303K / I336K	1	51	85	1 / 0	0,56	1,04
W1282X / 3849+10kbC->T	1	58	124	1 / 0	0,63	1,05

PS: pancreatic sufficient; PI: pancreatic insufficient; CI: circularity index; IR: intensity ratio